

The Effect of the Selection of a Function Approximating Static Characteristics on the Modelling of Electric Arc

Abstract: The article presents selected tapering functions useful when creating hybrid models and functions approximating static current-voltage characteristics of arc. The research work involved the formation and verification of families of static current-voltage characteristics with defined values of voltage ignition and the extension of approximating possibilities of the formulas through the use of tapering functions. The effective use of various functions approximating static characteristics in the modelling of dynamic states in the circuit with electric arc was verified through simulation.

Keywords: electric arc, static current-voltage characteristics, the Pentegov model

DOI: [10.17729/ebis.2020.6/4](https://doi.org/10.17729/ebis.2020.6/4)

Introduction

There are several types of mathematical models electric arc utilising static current-voltage characteristics including the Novikov-Schellhase model [1–4], the Pentegov model (developed along with Sidoretz) [5, 6] and the Mayr-Pentegov model [7, 8]. The above-presented sequence of the models corresponds to a decrease in the force of reduction assumptions and the improved adequacy in the mapping of physical processes in circuits with electric arc. The advantage of the above-named models is the at least two-stage process of parameter determination, enabling the significant simplification of diagnostic methods. The effectiveness of arc modelling is significantly affected by the approximating accuracy of the family of the static current-voltage characteristics of arc. The selection of a function approximating experimental characteristics depends on the power

of discharge (length of (voltage) column and current), the physicochemical conditions of arc burning (chemical composition of gas, pressure and the temperature of a gaseous environment), the selection of a mathematical model of arc etc. [9]. Because of numerous difficulties accompanying the precise diagnostics of electric discharge, the attempted obtainment of high approximation precision has its rational limitations. In the modelling of low-current arc, the proper mapping of arc voltage is of significant importance [2]. In the modelling of high-current arc, a crucial aspect may be the mapping of the flat or increasing fragment of a current-voltage characteristic. In turn, taking into account an appropriate value of residual conductance improves the stability of numerical simulations of processes in systems with electric arc [10].

Publications [11] discuss the use of functions approximating static characteristics

characterised by a relatively strong interaction between parameters defined in these functions. A relatively easy method enabling the reduction of the aforesaid interaction consists in using an appropriate tapering function [12]. In hybrid models [13], the application of tapering functions makes it possible to activate an appropriate submodel. Usually, such submodels contain various static current-voltage characteristics corresponding to low-current and high-current ranges. Because of the fact that in the Novikov-Schelhase, Pentegov-Sidoretz and Mayra-Pentegov models it is possible to select a static characteristic within the entire current range, it is also possible, as early as at the first stage of the building of the model, to associate fragments of functions approximating measurement data within low-current or high-current ranges. The increased complexity of approximating functions does not significantly affect the structure of macromodels utilising the Novikov-Schelhase or the Pentegov-Sidoretz models. However, because of the analytical determination of a derivative of static conductance in relation to squared current [7, 8], the aforesaid complexity could impede the application of the Mayr-Pentegov model. For this reason, in the research work discussed in this article, processes in circuits with electric arc were only simulated using the Pentegov model.

Tapering functions used for the creation of hybrid models and functions approximating static current-voltage characteristics of arc

Tapering functions are relatively commonly used in the creation of hybrid models of electric arc [13]. The most common form is the one forming the Gaussian curve

$$\varepsilon(i) = \exp\left(-\frac{i^2}{I_0^2}\right)$$

where I_0 defines ultimate model-switching current, A, corresponding to the value of ordinate $\varepsilon(I_0) = 1/e \approx 0.367879...$. The above-presented modification of the formula enables the more comfortable choice of submodel switching conditions

$$\varepsilon_i(i) = \exp\left(\ln(k_i) \frac{i^2}{I_0^2}\right)$$

Value k_i defines the ordinate of the point of the switching of function $\varepsilon(I_0) = k_i$, where $0 < k_i < 1$.

Figure 1 presents diagrams of tapering functions obtained using the Gaussian dependence and its modifications. Even greater possibilities of associating arc models into hybrid arc models are “offered” by the tapering function using power expressions having form [12],

$$\varepsilon(i) = \exp\left(-\frac{|i|^k}{I_0^k}\right)$$

where exponent $k > 0$. The above-presented function can be modified in a similar manner and adopt the following form

$$\varepsilon_i(i) = \exp\left(\ln(k_i) \frac{|i|^k}{I_0^k}\right)$$

Figure 2 presents diagrams of tapering functions obtained using exponential and power dependences.

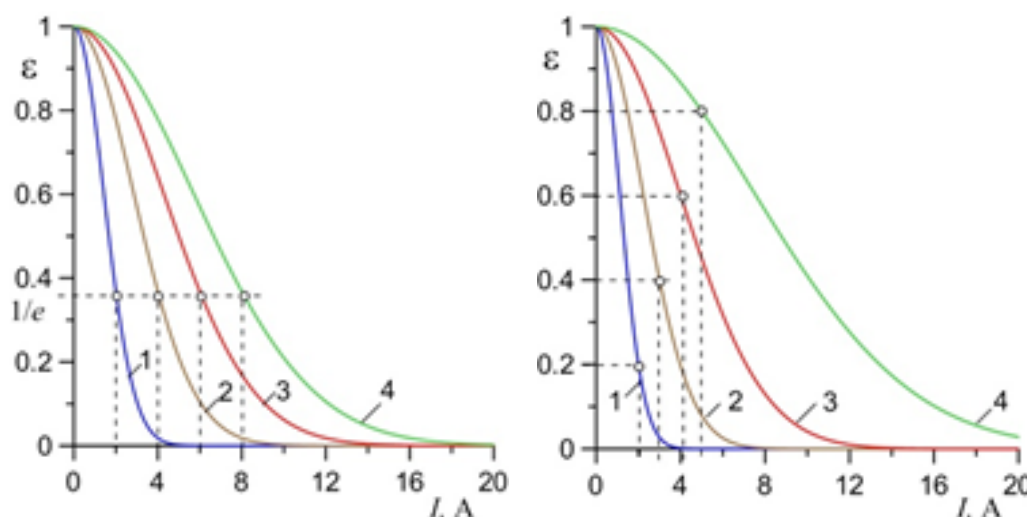


Fig. 1. Diagrams of tapering functions: a) generating Gaussian functions (1) (1 – $I_0 = 2$ A, 2 – $I_0 = 4$ A, 3 – $I_0 = 6$ A, 4 – $I_0 = 8$ A); b) generating modified Gaussian functions (2) (1 – $I_0 = 2$ A, $k_1 = 0.2$; 2 – $I_0 = 3$ A, $k_1 = 0.4$, 3 – $I_0 = 4$ A, $k_1 = 0.6$, 4 – $I_0 = 5$ A, $k_1 = 0.8$)

The above-presented diagrams justify the conclusion that the above-named tapering functions make it possible to both easily and extensively define the method of the switching of hybrid models or fragments of non-linear static current-voltage characteristics of arc.

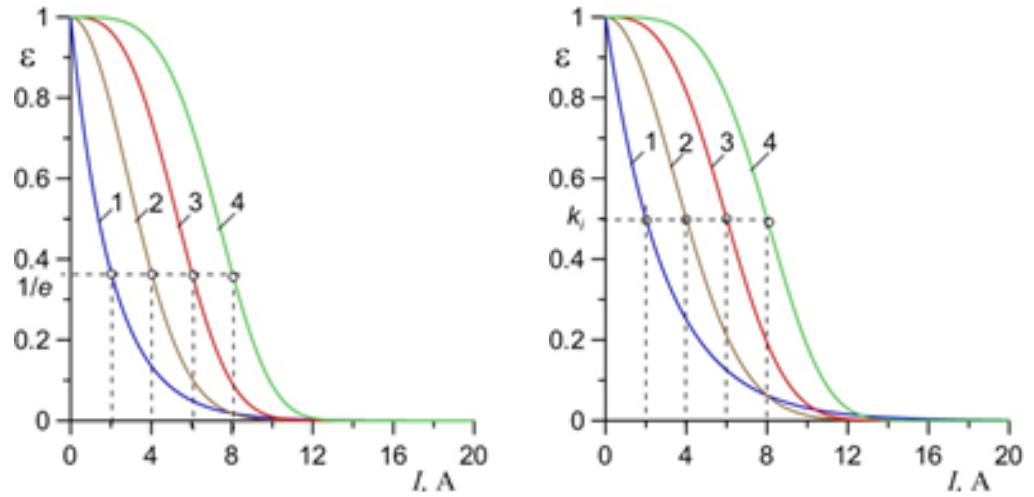


Fig. 2. Diagrams of tapering functions: a) expressed by formula (3) (1 – $I_0 = 2$ A, $k = 1$; 2 – $I_0 = 4$ A, $k = 2$; 3 – $I_0 = 6$ A, $k = 3$; 4 – $I_0 = 8$ A, $k = 4$); b) expressed by formula (4) ($k_i = 0.5$, 1 – $I_0 = 2$ A, $k = 1$, 2 – $I_0 = 4$ A, $k = 2$, 3 – $I_0 = 6$ A, $k = 3$, 4 – $I_0 = 8$ A, $k = 4$)

Static current-voltage characteristics of arc with the ordinary and the improved method of ignition voltage definition

Presented below are three cases of simplified functions approximating static current-voltage characteristics of arc. The aforesaid functions, taking into account the determinacy of arc ignition, were selected so that it would be possible to gradually increase the approximation potential of gathered measurement data, yet they were characterised by the relatively strong interaction of parameters. To weaken the aforesaid interaction, in each case it was additionally necessary to modify the approximating function thorough the application of a tapering function.

The first case of the approximation of a static current-voltage characteristic is the function containing components corresponding to low-current and high-current ranges

$$U(I) = \frac{P_M I}{I^2 + I_p^2} + U_C + R_p I$$

where P_M – constant parameter connected with power (and voltage ignition), W; I_M – constant parameter connected with the abscissa of ignition voltage, A; U_C – constant parameter connected with plateau voltage (of $R_p = 0$ Ω) within the high-current range, V; R_p – constant parameter connected with a rise on characteristics within the high-current range, Ω.

In such a case, residual conductance is expressed by the following formula

$$G_{re} = \frac{1}{\frac{P_M}{I_p^2} + R_p}$$

The interaction of the parameters of function (5) affects the determination of values of ignition voltage. The foregoing can be stated by analysing the following cases:

- if $U_C = 0$ V and $R_p = 0$ Ω, the extreme point has coordinates $(I_p, P_M/(2I_p))$;
- if $U_C > 0$ V and $R_p = 0$ Ω, the extreme point has coordinates $(I_p, P_M/(2I_p) + U_C)$;
- if $U_C > 0$ V and $R_p > 0$ Ω, the extreme point has approximate coordinates $(I_p, P_M/(2I_p) + U_C + R_p I_p)$.

In the latter case, the precise determination of the coordinates of the extreme point is possible but its notation could be extensive. Because of the relatively low value of parameter R_p and the relatively low value of current $I \approx I_p$, the effect of component $R_p I_p$ on the extreme point may not be high. Usually, component U_C is responsible for a significant increase in the value of ignition voltage, whereas component $R_p I$ is responsible for a slight increase in the value of ignition voltage and its slight shift towards lower current values.

In relation to (5), the modified approximating function with the reduced interaction of

parameters could have the following form

$$U(I) = \frac{P_M I}{I^2 + I_p^2} \varepsilon(I) + (U_C + R_p I) \cdot (1 - \varepsilon(I))$$

with additionally introduced $\varepsilon(I)$ – tapering function having properties: $\varepsilon(0) = 1$, $\varepsilon(\infty) = 0$. The application of the function significantly reduces the effect of parameters U_C and R_p on the value of ignition voltage. Approximately, residual conductance is as follows

$$G_{re} \cong \frac{I_p^2}{P_M}$$

Figure 3 presents the families of the static current-voltage characteristics of arc obtained using functions (5) and (7). It can be seen that in the second case the definition of parameters of in the low-current range is not only easier but also more effective.

In comparison with formula (6), more extensive approximating potential is that of the function having the following form

$$U(I) = U_s \left(\frac{I_s I}{I^2 + I_p^2} \right)^n + U_C + R_p I$$

where U_s , I_s – constant parameters connected with the value of ignition voltage; I_p – constant parameters connected with the abscissa of ignition voltage, A; n – constant exponent. The

remaining parameters U_C and R_p play the same role as previously. In this case, the residual conductance of arc depends on the value of exponent n in the following manner:

$$\text{if } n = 1, \quad G_{re} = \frac{1}{\frac{U_s I_s}{I_p^2} + R_p}$$

$$\text{if } n > 1, \quad G_{re} = 1/R_p.$$

The interaction of the parameters affects the determination of ignition voltage. The foregoing can be stated by analysing the following cases:

- if $U_C = 0$ V and $R_p = 0$ Ω , the extreme point has coordinates $(I_p, U_s I_s^n / (2 I_p^n))$;
- if $U_C > 0$ V and $R_p = 0$ Ω , the extreme point has coordinates $(I_p, U_s I_s^n / (2 I_p^n) + U_C)$;
- if $U_C > 0$ V and $R_p > 0$ Ω , the extreme point has approximate coordinates $(I_p, U_s I_s^n / (2 I_p^n) + U_C + R_p I_p)$. The justification of the above-presented notation is analogous to the previous case.

In relation to formula (9), the modified approximating function may adopt the following form

$$U(I) = U_s \left(\frac{I_s I}{I^2 + I_p^2} \right)^n \varepsilon(I) + (U_C + R_p I) \cdot (1 - \varepsilon(I))$$

Also in this case tapering function $\varepsilon(I)$ was introduced. The foregoing resulted in the significant reduction of the effect of parameters U_C

and R_p on the value of ignition voltage. Also in this case, the residual conductance of arc depends on the value of the exponent in the following manner:

$$\text{if } n = 1, \quad G_{re} \cong \frac{I_p^2}{U_s I_s}$$

$$\text{if } n > 1, \quad G_{re} \approx \infty \text{ S.}$$

Figure 4 presents the families of the static current-voltage characteristics of arc obtained using functions (9) and (10). It can be seen that in

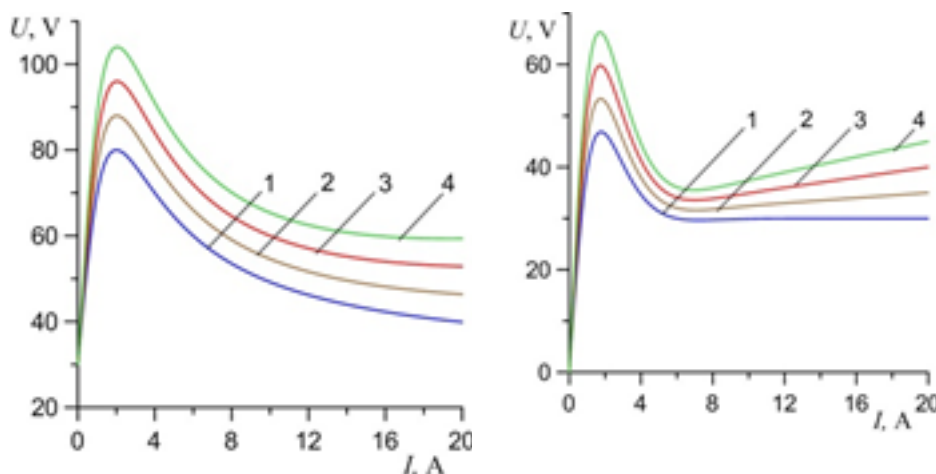


Fig. 3. Families of the static current-voltage characteristics of electric arc ($U_C = 30$ V, $I_p = 2$ A; 1 – $P_M = 200$ W, $R_p = 0$ Ω ; 2 – $P_M = 230$ W, $R_p = 0.25$ Ω ; 3 – $P_M = 260$ W, $R_p = 0.5$ Ω ; 4 – $P_M = 290$ W, $R_p = 0.75$ Ω): a) expressed by formula (5); b) expressed by formulas (7) and (2) ($k_i = 0.3$, $I_0 = 5$ A)

accordance with (10) the definition of parameters of in the low-current range is not only easier but also more effective.

When modelling electric arc it is sometimes preferred to use the approximations of static current-voltage characteristics using exponential functions [1–3]. An example of the above-named simplified approximation is dependence

$$U(I, p) = U_p \left(\frac{I}{I_p} \right)^n \exp \left[1 - \left(\frac{I}{I_p} \right)^n \right] + U_C + R_p I$$

where U_p – component of ignition voltage, V; I_p – abscissa of defined ignition voltage, A; n – constant exponent. The remaining parameters U_C and R_p play the same role as previously. In this case, the residual conductance of arc does not depend on the value of exponent n and is $G_{re} = 1/R_p$.

The interaction of the parameters affects the determination of ignition voltage. The foregoing can be stated by analysing the following cases:

- if $U_C = 0$ V and $R_p = 0$ Ω , the extreme point has coordinates (I_p, U_p) ;
- if $U_C > 0$ V and $R_p = 0$ Ω , the extreme point has coordinates $(I_p, U_p + U_C)$;
- if $U_C > 0$ V and $R_p > 0$ Ω , the extreme point has approximate coordinates $(I_p, U_p + U_C + R_p I_p)$. The justification of the above-presented notation is analogous to the previous case.

In relation to (11), the modified approximating function with the reduced interaction of parameters could adopt the following form:

$$U(I, p) = U_p \left(\frac{I}{I_p} \right)^n \exp \left[1 - \left(\frac{I}{I_p} \right)^n \right] \varepsilon(I) + (U_C + R_p I) \cdot (1 - \varepsilon(I))$$

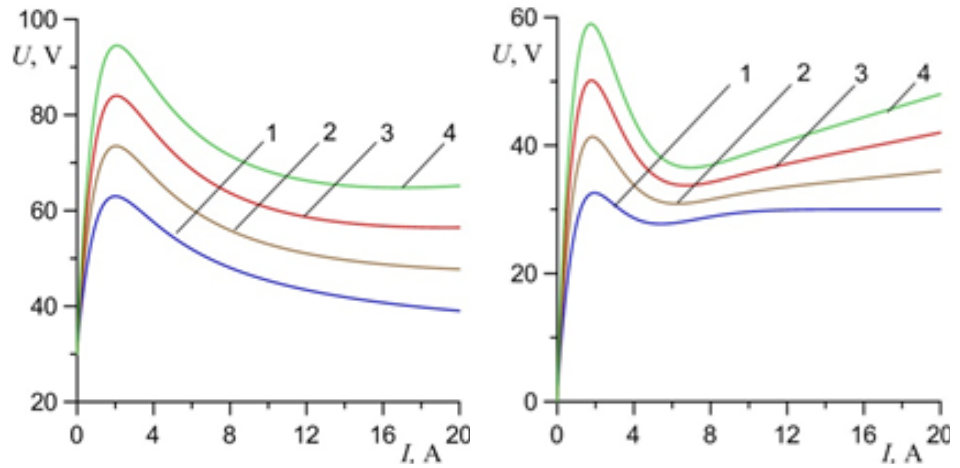


Fig. 4. Families of the static current-voltage characteristics of electric arc ($U_C = 30$ V, $I_p = 2$ A, $I_s = 1$ A, $n = 0,8$): a) expressed by formula (9) (1 – $U_s = 100$ V, $R_p = 0$ Ω ; 2 – $U_s = 130$ V, $R_p = 0,3$ Ω ; 3 – $U_s = 160$ V, $R_p = 0,6$ Ω ; 4 – $U_s = 190$ V, $R_p = 0,9$ Ω); b) expressed by formulas (10) and (4) ($k = 2$, $k_i = 0,4$, $I_0 = 5$ A; 1 – $U_s = 100$ V, $R_p = 0$ Ω ; 2 – $U_s = 130$ V, $R_p = 0,3$ Ω ; 3 – $U_s = 160$ V, $R_p = 0,6$ Ω ; 4 – $U_s = 190$ V, $R_p = 0,9$ Ω)

Also in this case tapering function $\varepsilon(I)$ was introduced. The foregoing resulted in the significant reduction of the effect of parameters U_C and R_p on the value of ignition voltage. Also in this case, the residual conductance of arc does not depend on the value of exponent n and is $G_{re} \approx \infty$.

Figure 5 presents the families of the static current-voltage characteristics of arc obtained using functions (11) and (12). It can be seen that the determination of parameters of within the low-current range is easier and more effective.

It possible to extend function (12) and, as a result, obtain the higher accuracy of approximation (as was the case with works [1–3]). However, because of unavoidable and relatively large diagnostics errors, such an action may not bring significant advantages.

It is also possible to reduce approximating functions (7), (10) or (12) by ignoring tapering function $\varepsilon(I)$ in the first components. They contain functions decreasing within the high-current range. However, the above-named action may worsen the quality of approximation. Such a parameter of static characteristics as I_p is connected with the dynamic processes of current passing through the zero value. For this reason, the determination of the aforesaid parameter should take place during AC powering [10].

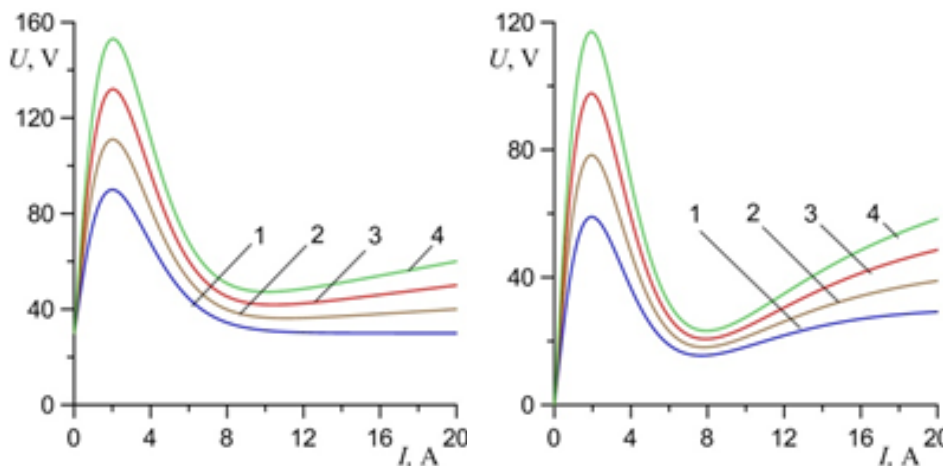


Fig. 5. Families of the static current-voltage characteristics of electric arc ($U_C = 30$ V, $I_p = 2$ A, $n = 1, 2$): a) expressed by formula (11) (1 – $U_p = 60$ V, $R_p = 0$ Ω ; 2 – $U_p = 80$ V, $R_p = 0.5$ Ω ; 3 – $U_p = 100$ V, $R_p = 1$ Ω ; 4 – $U_p = 120$ V, $R_p = 1.5$ Ω); b) expressed by formulas (12) and (2) ($I_0 = 5$ A, $k_i = 0.8$; 1 – $U_p = 60$ V, $R_p = 0$ Ω ; 2 – $U_p = 80$ V, $R_p = 0.5$ Ω ; 3 – $U_p = 100$ V, $R_p = 1$ Ω ; 4 – $U_p = 120$ V, $R_p = 1.5$ Ω)

Simulations of processes in the circuit using the Pentegov model of electric arc

The creation of the Pentegov mathematical model of electric involves energy balance and the use of reduction assumptions [5, 6]. Instead of actual arc, the above-named model involves hypothetic arc, where the conductance of the arc column is defined as the function of fictitious (virtual) state current $i_\theta(t)$, changing along with specific time constant θ . Arc in the circuit is modelled by means of a two-terminal network, which is balanced in terms of energy, first-order thermally inert, non-linear, stationary and electrically inertialess. In accordance with related assumptions, the current and voltage of the model satisfy the condition

$$\frac{i}{u} = \frac{i_\theta}{U} = g$$

where $U(I)$ – static current-voltage characteristic of arc. Based on the equation of power balance in the column

$$\frac{dQ}{dt} + Ui_\theta = ui$$

where dQ/dt – derivative of the change in the internal energy of plasma, ui – supplied electric energy; Ui_θ – electric power dissipated from

the column), it is possible to obtain a 1st order non-linear differential equation describing the dynamics of changes in state current $i_\theta(t)$, corresponding to changes in plasma temperature

$$\theta \frac{di_\theta^2}{dt} + i_\theta^2 = i^2$$

Formulas (13), (14) and (15) can be used to create a macromodel of arc in a simulation software programme. Then, non-linear resistance is mapped by a controlled volt-

age source having the following value

$$u = \frac{U(i_\theta)}{i_\theta} i$$

and the arrow directed oppositely to current flow [4]. Because of the fact that, similar to plasma temperature and arc column conductance, state current is greater than zero, the above-presented functions approximating static current-voltage characteristics can be used directly, i.e. without the necessity of calculating momentary current.

The correctness of the above-presented mathematical dependences was verified by creating macromodels of arc using selected functions approximating static current-voltage characteristics. To this end, it was necessary to use the source of sinusoidal current having amplitude $I_m = 200$ A and frequency $f = 50$ Hz, ensuring the stable burning of arc. The adopted constant sum of near-electrode voltage drops was $U_{AK} = 18$ V. The parameters of the models were adjusted so that it would be possible to demonstrate the effect of the parameters on the shapes of the dynamic characteristics of arc.

Figure 6a presents the dynamic current-voltage characteristics of arc utilising the generalised form of the approximating function with the defined value of ignition voltage (5).

The above-presented function was modified by the introduction of the tapering function, facilitating the determination of the maximum value of ignition voltage (Fig. 6b).

Figure 7 presents the dynamic current-voltage characteristics of arc utilising an even more general (if compared with that presented in Fig. 6) form of the approximating function with the defined value of ignition voltage. The reduction of the interaction of parameters when determining the above-named voltage was obtained using formula (1) (see Figure 7b).

Figure 8 presents the dynamic current-voltage characteristics of arc utilising the approximating function containing the exponential function. In this case, the first component of formula (11) enables the determination of ignition voltage without interaction with current I_p . However, the remaining components affect the value of ignition voltage. The application of the tapering function enables the reduction of the aforesaid influence.

Conclusions

1. Selected models of AC electric arc involve the use of static current-voltage characteristics which may be characterised by the interaction of parameters.

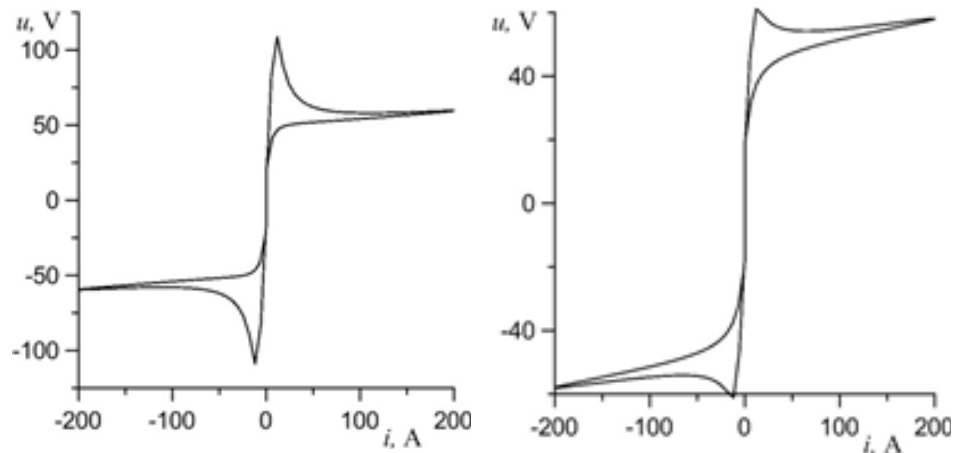


Fig. 6. Dynamic current-voltage characteristics of arc ($P_M = 300\text{W}$, $U_C = 30\text{ V}$, $R_p = 0.05\ \Omega$, $I_p = 2\text{ A}$): a) developed using the static current-voltage characteristic (5) and b) developed using the static current-voltage characteristic defined by (7) and (2) ($I_0 = 5\text{ A}$, $k_i = 0.3$)

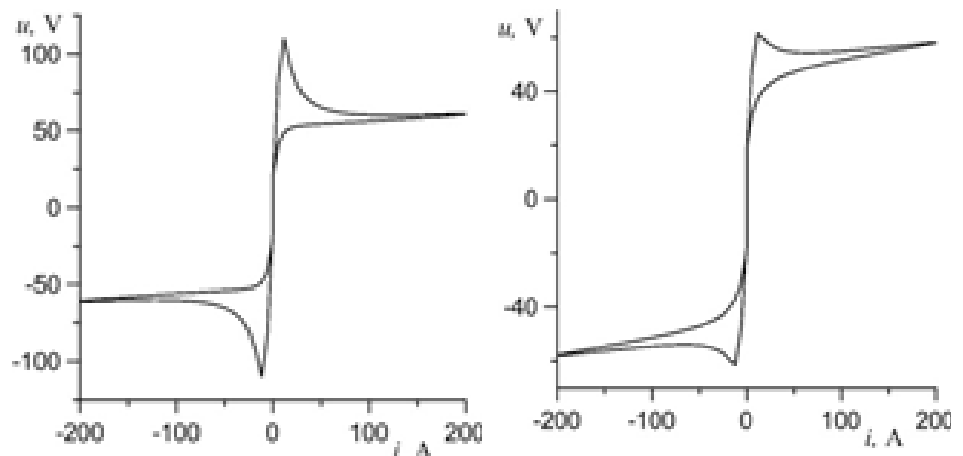


Fig. 7. Dynamic current-voltage characteristics of arc ($U_s = 200\text{ V}$, $I_s = 1\text{ A}$, $n = 0.8$, $U_C = 30\text{ V}$, $R_p = 0.05\ \Omega$, $I_p = 2\text{ A}$): a) developed using the static current-voltage characteristic (9) and b) developed using the static current-voltage characteristic defined by (10) and (4) ($I_0 = 5\text{ A}$, $k = 2$, $k_i = 0.4$)

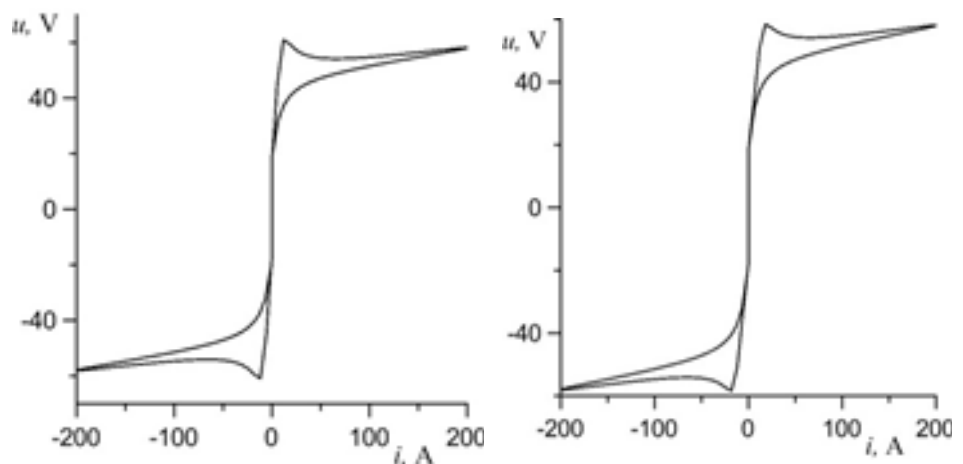


Fig. 8. Dynamic current-voltage characteristics of arc ($U_p = 120\text{ V}$, $I_p = 1\text{ A}$, $n = 1,2$, $U_C = 30\text{ V}$, $R_p = 0,05\ \Omega$): a) developed using the static current-voltage characteristic (9) and b) developed using the static current-voltage characteristic defined by (10) and (4) ($I_0 = 5\text{ A}$, $k = 2$, $k_i = 0.4$)

2. The introduction of tapering functions to functions approximating static current-voltage characteristics makes it possible to reduce interaction between the parameters, improving the clarity of description and the accuracy of calculations.

3. The above-presented tapering functions can be used for generating hybrid models electric arc.

References

- [1] Marciniak L.: Implementacje modeli łuku ziemnozwarciowego w programach PSCAD i Matlab/Simulink. *Przegląd Elektrotechniczny*, 2012, no. 9a, pp. 126–129.
- [2] Marciniak L.: Model of the arc earth-fault for medium voltage networks. *Central European Journal of Engineering*. 2011, no. 2, pp. 168–173.
- [3] Marciniak L.: Modele dynamiczne łuku zwarcia doziemnego. *Archives of Energetics*, 2007, no. 37, pp. 357–367
- [4] Sawicki A.: Modele matematyczne różniczkowe i całkowite w makromodelowaniu łuku elektrycznego z wykorzystaniem źródeł sterowanych napięciowych i prądowych. Cz.2. Wybrane modele matematyczne łuku z jawnie zdefiniowanymi charakterystykami napięciowo-prądowymi statycznymi. *Biuletyn Instytutu Spawalnictwa* 2020, no. 1, pp. 21–25.
- [5] Pientegov I. V.: Matematicheskaja model stolba dinamiczeskoj elektriceskoj dugi. *Avtomaticzeskaja svarka*, 1976, vol. 279, no. 6, pp. 8–12.
- [6] Pientegov I. V., Sidoriec V. N.: Sravnitelnyj analiz modelej dinamiczeskoj svarocznoj dugi. *Avtomaticzeskaja svarka*, 1989, vol. 431, no. 2, pp. 33–36. Pentegov I. V. and V. N. Sydorets: Comparative analysis of models of dynamic welding arc. *The Paton Welding Journal*, 2015, no. 12, pp. 45–48.
- [7] Sawicki A.: The universal Mayr-Pentegov model of the electric arc. *Przegląd Elektrotechniczny (Electrical Review)*, 2019, vol. 94, no. 12, pp. 208–211. (doi:10.15199/48.2019.12.47)
- [8] Sawicki A.: Modele Mayra-Pentegova łuku elektrycznego z wybranymi charakterystykami napięciowo-prądowymi statycznymi. *Biuletyn Instytutu Spawalnictwa* 2020, no. 3, pp. sprawdzić po wydaniu)
- [9] Sawicki A.: Aproksymacje charakterystyk napięciowo-prądowych łuku urządzeń elektrotechnologicznych. *Biuletyn Instytutu Spawalnictwa*, 2013, no. 6, pp. 58–68.
- [10] Sawicki A.: Klasyczne i zmodyfikowane modele matematyczne łuku elektrycznego. *Biuletyn Instytutu Spawalnictwa*, 2019, no. 4, pp. 73–76.
- [11] Sawicki A.: Modele matematyczne różniczkowe i całkowite w makromodelowaniu łuku elektrycznego z wykorzystaniem źródeł sterowanych napięciowych i prądowych. Cz. 1. Warianty makromodeli łuku elektrycznego zadawane przez różne postacie równań różniczkowych lub całkowych. *Biuletyn Instytutu Spawalnictwa*, 2019, no. 6, pp. 67–72.
- [12] Sawicki A.: Funkcje wagowe w modelach hybrydowych łuku elektrycznego. *Śląskie Wiadomości Elektryczne*, 2012, no. 5, pp. 15–19.
- [13] King-Jet Tseng, Yaoming Wang D.: Mahinda Vilathgamuwa: An Experimentally Verified Hybrid Cassie-Mayr Electric Arc Model for Power Electronics Simulations. *IEEE Transactions on Power Electronics*, vol. 12, no. 3, pp. 429–436, <http://dx.doi.org/10.1109/63.575670>